Thermochromism of the Crystals of 2,3-Bis(phenylthio)-1,4-naphthoquinone

Masashi Tanaka,* Hisahiro Hayashi,† Shingo Matsumoto,†† Setsuo Kashino,†† and Kouichi Mogi†††

Department of Natural Science Informatics, School of Informatics and Sciences, Nagoya University, Chikusa-ku, Nagoya 464-01

†Division of Informatics for Science, Graduate School of Human Informatics, Nagoya University, Chikusa-ku, Nagoya 464-01

††Department of Chemistry, Faculty of Science, Okayama University, Tsushima, Okayama 700

†††Institute for Molecular Science, 38 Saigo-naka, Aza, Myodaiji-cho, Okazaki 444

(Received September 9, 1996)

The crystals of 2,3-bis(phenylthio)-1,4-naphthoquinone have the dimorphs of red and violet forms. The crystal structures of a monoclinic form (violet form) and an orthorhombic form (red form) have been determined by the X-ray diffraction method. In the orthorhombic form, two phenylthio groups are located on the same side of the naphthoquinone plane, while in the monoclinic form one phenylthio group is located on the naphthoquinone plane and the other phenylthio group is located under the plane. The violet form changes to the red form upon heating. The thermochromism of these crystals was studied, based on the crystal structures of the dimorphs and the solid state CP-NMR and IR and visible absorption spectra and the differential scanning calorimetry together with the theoretical analysis of the data of IR and visible absorption spectra.

A number of organic compounds undergo reversible color changes by the alternation of the molecular structure with temperature. However, a few organic compounds in the solid phase can undergo chemical changes which are in many respects unparalleled for the same molecules in a solution. For example, 2-(4-methoxyphenyl)-1,4-benzoquinone crystallizes as both a yellow and a red solid, and the yellow solid undergoes a thermal reaction to give the red solid.[1] The irreversible thermochromism of the crystals of 2,3-bis(*p*-chlorophenylthio)-1,4-naphthoquinone (Cl-BPNQ) changes the red form to the dark red form upon heating.[2] The yellow and green forms of picrates salts with 2-iodoaniline show the thermochromism and change to the red crystals upon heating.[3] Such thermochromism in the solid phase occurs due to the variation of the charge transfer interaction in the crystal. Many compounds with the properties of the phase transition by the temperature, light and pressure have possible applications to molecular devices or indicators. The structural and spectral studies of such molecules and molecular aggregates are important to the research of the functionality of the molecules. In the present paper, we report the irreversible thermochromism of the crystals of 2,3-bis(phenylthio)-1,4-naphthoquinone (BPNQ) and discuss the change of the molecular structure by the results of the X-ray analysis and the CP-NMR for two forms. We describe the mechanism of the phase transition by the measurement of the variable temperature IR absorption spectra, and we elucidate the chromic phenomena by the results of the visible absorption spectra, together with some theoretical analysis.

Experimental

Synthesis. BPNQ was prepared by the method of Miyaki and Ikeda[4] and Fieser and Brown.[5] BPNQ gave two kinds of crystals according to the conditions of recrystallization, the unstable one of red needles (red form) for the slow descent of temperature with stirring the 2-propanol solution, and the stable one of violet prisms (violet form) by evaporating or cooling the ethylacetate solution.[4]

Measurements. The ^{13}C NMR solution spectra were taken by the JNM 270 MHz ^{1}H NMR and 400 MHz PC NMR spectrometers and the CP/MAS NMR solid state spectra by the JEOL CMX300, respectively. Thermal analyses were carried out using a Shimadzu differential scanning calorimeter (DSC) and thermogravimetry analysis (TGA) at heating rate of 10 °C min^{-1} under N_2 gas. The IR absorption spectra of the single crystal were recorded using a JASCO FTIR VALOR III with the hotplate FP82HT. The visible absorption spectra were taken using an absorption microphotometer made in our laboratory.[6]

X-Ray Structure Analysis. Experimental details and crystal data for violet and red forms are listed in Table 1.[7] The reflection data were measured on a Rigaku AFC-5R four circle diffractometer with graphite monochromated Mo $K\alpha$ radiation ($\lambda = 0.71073$ Å) at 50 kV and 200 mA. Lattice parameters were determined with 25 reflections in the range $20 < 2\theta < 22°$. Intensities were measured by using ω–2θ scan technique where the scan speed was 6° min^{-1} in ω. The scan ranges in ω were $(0.84 + 0.30 \tan\theta)°$ for the violet form and $(1.78 + 0.30 \tan\theta)°$ for the red form. Background was measured for 4 s on either side of the peak. Three standard reflections were monitored during the data collection for every 97

Table 1. Crystal Data of 2,3-Bis(phenylthio)-1,4-naphthoquinone (Violet and Red Forms)

	Violet form	Red form
M_r	374.47	374.47
Morphology	Prismatic	Prismatic
Specimen/mm	$0.25\times0.15\times0.50$	$0.35\times0.20\times0.50$
Crystal system	Monoclinic	Orthorhombic
Space group	$P2_1/n$	$Pmn2_1$
a/Å	5.159(2)	21.282(7)
b/Å	10.436(2)	5.269(4)
c/Å	32.834(6)	8.141(4)
β/°	93.47(2)	
Z	4	2
V/Å^{-3}	1765(1)	913(1)
D_{cal}/g cm^{-3}	1.410	1.362
$F(000)$	776	388
μ/mm^{-1}	0.30	0.29
$2\theta_{max}$/°	52.0	48.0
Range of h, k, l	$0\leqq h\leqq6$	$0\leqq h\leqq27$
	$0\leqq k\leqq13$	$-1\leqq k\leqq6$
	$-42\leqq l\leqq42$	$0\leqq l\leqq10$
Fluctuation of standard refs./%	0.8	0.9
R_{int}	0.017	0.072
Number of unique refs. used	1779	567
Number of parameters	291	117
R/wR	0.060/0.052	0.068/0.047
S	1.86	1.95
$(\Delta/\sigma)_{max}$	0.68	0.07
$\Delta\rho_{max}$/e Å^{-3}	0.27	0.26
$\Delta\rho_{max}$/e Å^{-3}	−0.34	−0.30

reflections. Correction for the Lorentz and polarization effects were applied, but no correction was applied for the absorption effect. The structures were solved by a direct method MITHRIL[8] and refined by a full-matix least-squares using unique reflections with I_o larger than $3\sigma(I_o)$. The quantity minimized was $\Sigma w(|F_o|-|F_c|)^2$ where w refers to weights, $\sigma^{-2}(F_o)$. The non-hydrogen atoms were refined anisotropically. The hydrogen atoms of the violet form were refined isotropically. For the red form the positional parameters of the hydrogen atoms were calculated by assuming the usual geometry and their isotropic displacement parameters were assumed to be the same as the equivalent displacement parameters of the atoms to which they were attached. Atomic scattering factors were taken from International Tables for X-Ray Crystallography.[9] Computations were carried out by using TEXAN[10] at the X-Ray Laboratory of Okayama University.

Theoretical Analysis. All ab initio molecular orbital calculations were performed with the GAUSSIAN 94 program.[11] The numerical calculations were carried out on IBM RS/6000 590 and SP2 parallel computers and NEC SX-3 supercomputer at the Institute for Molecular Science (IMS) computer center. The geometries of these two isomers were fully optimized at the RHF/3-21G* level and one point calculations were performed with the second order-Møller–Plesset (MP2) calculations on the optimized geometry. Excitation energies for each isomer were determined by the configuration interaction single (CIS) method. Vibrational analyses were also performed to characterize the stationary points.

Results and Discussion

Crystal and Molecular Structures. Final atomic parameters for the violet and red forms are listed in Table 2. In the red form, the BPNQ molecule occupies a special position 2a of $Pnm2_1$. Thus the molecule has a C_s symmetry in the crystal and a half of the molecule constitutes an asymmetric unit. The ORTEP drawing and the numbering of atoms are shown in Fig. 1. The numbering system of the asymmetric unit of the red form is the same as that of the corresponding part of the violet form.[12] The C(2) and C(3) are not equivalent for the violet form, while the corresponding C atoms in the red form C(2) and C(2′) are related by a mirror plane.

The bond lengths and bond angles are listed in Tables 3 and 4, respectively. The low precisions of the atomic parameters obtained for the red form limit any detailed comparison of the

Table 2. Fractional Atomic Coordinates and Equivalent Isotropic Displacement Parameters (Å^2) of Violet Form (a) and Red Form (b)

Atom	x	y	z	B_{eq}[a]
(a) Violet form				
S(1)	0.7527(5)	0.0335(2)	0.93426(5)	7.5(1)
S(2)	1.1598(5)	0.2317(1)	0.90839(5)	6.6(1)
O(1)	0.532(1)	−0.1151(4)	0.8622(1)	5.2(3)
O(2)	1.338(1)	0.1723(4)	0.8245(1)	5.3(3)
C(1)	0.723(1)	−0.0591(5)	0.8546(2)	3.8(3)
C(2)	0.864(1)	0.0321(5)	0.8846(1)	3.8(3)
C(3)	1.028(1)	0.1194(5)	0.8728(2)	4.2(3)
C(4)	1.152(1)	0.1087(5)	0.8323(2)	3.7(3)
C(5)	1.139(1)	−0.0023(7)	0.7651(2)	4.5(4)
C(6)	1.048(2)	−0.0946(7)	0.7382(2)	5.0(4)
C(7)	0.859(2)	−0.1740(7)	0.7493(2)	5.2(4)
C(8)	0.740(1)	−0.1622(5)	0.7868(2)	4.1(3)
C(9)	0.843(1)	−0.0694(5)	0.8140(2)	3.4(3)
C(10)	1.037(1)	0.0113(5)	0.8032(2)	3.3(3)
C(11)	0.740(1)	−0.1304(5)	0.9484(2)	4.4(3)
C(12)	0.925(2)	−0.2188(7)	0.9369(2)	4.9(4)
C(13)	0.912(2)	−0.3425(7)	0.9523(2)	5.8(5)
C(14)	0.733(2)	−0.3739(8)	0.9794(2)	5.5(4)
C(15)	0.554(2)	−0.2853(7)	0.9906(2)	5.4(4)
C(16)	0.556(1)	−0.1640(7)	0.9746(2)	4.7(4)
C(21)	1.174(1)	0.3762(5)	0.8799(2)	3.8(3)
C(22)	0.971(1)	0.4108(6)	0.8520(2)	4.4(3)
C(23)	0.983(1)	0.5308(6)	0.8333(2)	4.6(4)
C(24)	1.181(2)	0.6129(6)	0.8447(2)	4.8(4)
C(25)	1.376(2)	0.5786(6)	0.8730(2)	4.7(4)
C(26)	1.372(1)	0.4585(6)	0.8905(2)	4.4(3)
(b) Red form				
S(1)	0.0729(1)	0.4440(4)	0.3663	7.1(1)
O(1)	0.1239(3)	0.795(2)	0.629(1)	8.1(4)
C(1)	0.0687(5)	0.815(2)	0.611(1)	6.3(6)
C(2)	0.0332(3)	0.661(2)	0.487(1)	5.2(4)
C(7)	0.0323(4)	1.349(2)	0.900(1)	7.7(7)
C(8)	0.0635(4)	1.179(2)	0.803(1)	6.0(5)
C(9)	0.0322(3)	1.009(2)	0.708(1)	4.2(4)
C(11)	0.1378(5)	0.622(2)	0.288(1)	5.2(6)
C(12)	0.1277(5)	0.830(2)	0.196(2)	6.0(6)
C(13)	0.1765(7)	0.966(2)	0.125(2)	8.5(8)
C(14)	0.2353(6)	0.869(2)	0.151(2)	8(1)
C(15)	0.2476(5)	0.661(3)	0.238(2)	9.0(9)
C(16)	0.1973(5)	0.528(2)	0.312(1)	6.7(6)

a) $B_{eq}=(8\pi^2/3)\sum_i\sum_j U_{ij}a_i^*a_j^*\boldsymbol{a}_i\cdot\boldsymbol{a}_j$.

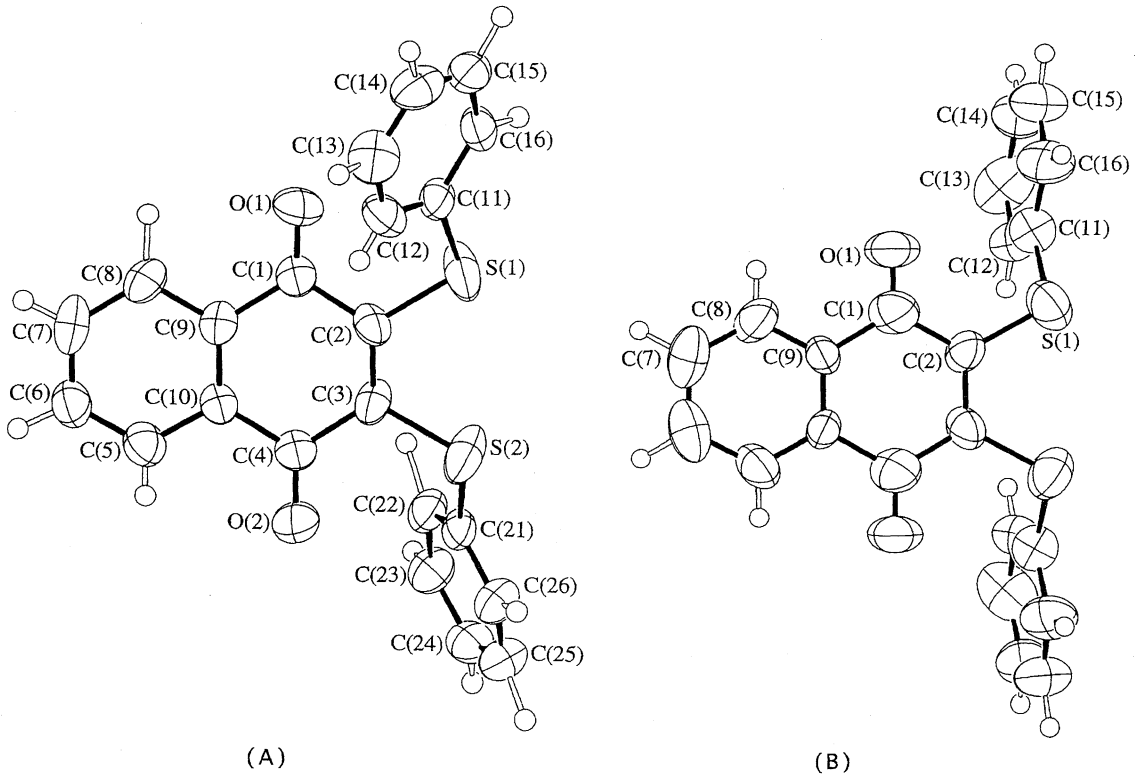

Fig. 1. Displacement ellipsoid plots with atomic numbering for (A) violet form and (B) red form. Ellipsoids of 50% probability are drawn for non-H atoms. H-atoms are represented as spheres equivalent to $B = 1.0$ Å^2.

Table 3. Bond Lengths (l/Å) with Their esd's in Parenthese

	Violet form	Red form
S(1)–C(2)	1.762(5)	1.73(1)
S(1)–C(11)	1.774(6)	1.79(1)
S(2)–C(3)	1.764(6)	—
S(2)–C(21)	1.780(5)	—
O(1)–C(1)	1.185(7)	1.188(9)
O(2)–C(4)	1.206(6)	—
C(1)–C(2)	1.520(8)	1.50(1)
C(1)–C(9)	1.509(7)	1.51(1)
C(2)–C(3)[a]	1.318(7)	1.41(1)
C(3)–C(4)	1.514(7)	—
C(4)–C(10)	1.494(7)	—
C(5)–C(6)	1.370(9)	—
C(5)–C(10)	1.396(7)	—
C(6)–C(7)[a]	1.346(9)	1.38(2)
C(7)–C(8)	1.414(8)	1.37(1)
C(8)–C(9)	1.398(7)	1.36(1)
C(9)–C(10)[a]	1.371(7)	1.37(1)
C(11)–C(12)	1.394(8)	1.35(1)
C(11)–C(16)	1.368(8)	1.37(1)
C(12)–C(13)	1.390(9)	1.39(1)
C(13)–C(14)	1.36(1)	1.37(2)
C(14)–C(15)	1.372(9)	1.34(2)
C(15)–C(16)	1.371(8)	1.41(1)
C(21)–C(22)	1.398(8)	—
C(21)–C(26)	1.361(8)	—
C(22)–C(23)	1.398(8)	—
C(23)–C(24)	1.369(9)	—
C(24)–C(25)	1.375(9)	—
C(25)–C(26)	1.381(8)	—

a) Read C(3) as C(2′), C(10) as C(9′) and C(6) as C(7′) for red form. A prime denotes an atom related by a mirror plane.

bond lengths and angles in both forms. However, a quinonoid character is remarkable for the quinone rings in both forms. The O atoms of the quinone ring deviates from the plane of the 1,4-naphthoquinone (NQ) ring: O(1) 0.273(9) Å and O(2) 0.14(1) Å in the violet forms; O(1) 0.28(2) Å in the red form. Such non-planarity of the quinone ring in BPNQ was also found in Cl-BPNQ,[2] although many naphthoquinones have planarity.[13,14]

Characteristic features of the molecular conformation of BPNQ in both forms are compared in Fig. 2 and Table 5. As seen from Fig. 2, in the violet form one phenylthio group is located on the NQ plane and the other phenylthio group is located under this plane (*Anti*-BPNQ). In the red form both thiophenyl groups are located on the same side of the plane (*Syn*-BPNQ). In the violet form the values of the torsion angles around C(2)–S(1) are similar to those around C(3)–S(2) (Table 5). This is also the case for the torsion angles around S(1)–C(11) and those around S(2)–C(21). This fact shows that the BPNQ molecule has a pseudo C_2 symmetry in the violet form. It is of note that absolute values of the corresponding torsion angles around C(2)–S(1) for both forms are close to each other. A significant difference in the orientation of the benzene ring plane with respect to the plane of the NQ ring in both forms is seen from the torsion angles C(2)–S(1)–C(11)–C(12) in both forms.

Projections of the crystal structures along the shortest axes for both forms are shown in Fig. 3. The dimensions of these axes in both forms are close to each other. The BPNQ molecules are stacked along these axes, respectively, in both forms. The NQ rings of the stacking molecules are

Table 4. Bond Angles (ϕ/°) with Their esd's in Parentheses

	Violet form	Red form
C(2)–S(1)–C(11)	104.6(3)	103.5(4)
C(3)–S(2)–C(21)	103.9(3)	—
O(1)–C(1)–C(2)	122.9(5)	123(1)
O(1)–C(1)–C(9)	122.8(6)	120(1)
C(2)–C(1)–C(9)	114.3(6)	117.4(8)
S(1)–C(2)–C(1)	115.8(5)	119.5(6)
S(1)–C(2)–C(3)[a)]	121.1(4)	119.3(3)
C(1)–C(2)–C(3)[a)]	122.2(5)	120.4(5)
S(2)–C(3)–C(2)	119.6(4)	—
S(2)–C(3)–C(4)	117.6(5)	—
C(2)–C(3)–C(4)	121.5(5)	—
O(2)–C(4)–C(3)	122.1(6)	—
O(2)–C(4)–C(10)	122.0(5)	—
C(3)–C(4)–C(10)	115.9(5)	—
C(6)–C(5)–C(10)	121.0(7)	—
C(5)–C(6)–C(7)	119.0(7)	—
C(6)–C(7)–C(8)[a)]	122.7(7)	119.0(6)
C(7)–C(8)–C(9)	116.7(7)	121.6(9)
C(1)–C(9)–C(8)	117.0(6)	119.6(8)
C(1)–C(8)–C(10)[a)]	121.9(5)	121.0(5)
C(8)–C(9)–C(10)[a)]	121.0(5)	119.4(5)
C(4)–C(10)–C(5)	119.0(6)	—
C(4)–C(10)–C(9)	121.6(5)	—
C(5)–C(10)–C(9)	119.4(6)	—
S(1)–C(11)–C(12)	122.1(5)	120.1(9)
S(1)–C(11)–C(16)	116.7(5)	118.3(8)
C(12)–C(11)–C(16)	120.9(6)	121(1)
C(11)–C(12)–C(13)	117.8(7)	122(1)
C(12)–C(13)–C(14)	120.8(8)	115(1)
C(13)–C(14)–C(15)	120.5(7)	125(1)
C(14)–C(15)–C(16)	119.9(7)	119(1)
C(11)–C(16)–C(15)	120.0(7)	117.5(9)
S(2)–C(21)–C(22)	120.6(5)	—
S(2)–C(21)–C(26)	117.0(5)	—
C(22)–C(21)–C(26)	121.7(5)	—
C(21)–C(22)–C(23)	117.8(6)	—
C(22)–C(23)–C(24)	119.5(7)	—
C(23)–C(24)–C(25)	121.8(7)	—
C(24)–C(25)–C(26)	119.1(7)	—
C(21)–C(26)–C(25)	119.8(6)	—

a) Read C(3) as C(2′), C(10) as C(9′) and C(6) as C(7′) for red form. A prime denotes an atom related by a mirror plane.

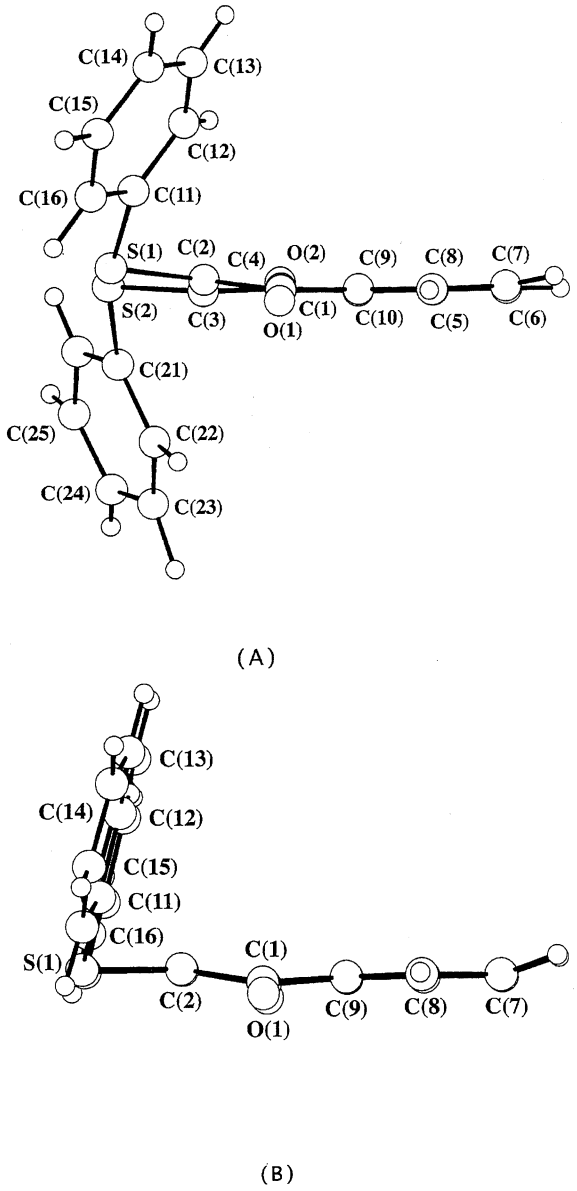

Fig. 2. Side views of the molecule in (A) the violet form and (B) the red form.

partially overlapped. However, there are no strong intermolecular interactions: The shortest interatomic distances are 3.165(7) Å for C(4)···O(1) $(1+x, y, z)$ in the violet form and 3.49(1) Å for C(7)···C(1) $(x, 1+y, z)$ in the red form. As seen from Fig. 3, the molecules are arranged along $\langle 0\,1\,0\rangle$ to form a chain in the violet form. A similar chain is formed along $\langle 1\,0\,1\rangle$ in the red form. The arrangement of the chains in Fig. 3 shows that the structure of the violet form may be changed to the structure of the red form by rotational and translational displacements of the molecules in the neighboring chains. The rotational displacements may amount to about 120 and 180° for the molecules in the neighboring chains related by a two-fold axis and a center of symmetry, respectively, but these may feasibly be attained by a concerted conformational change around the C–S bonds. The translational displacement is estimated to be less than about 3 Å for the neighboring molecules.

Thermal Studies. The violet form of BPNQ crystal is stable and the red form is unstable. The violet form changes irreversibly to the red form at about 108.5 °C upon heating, while the red form does not change upon cooling. DSC under nitrogen gas, presented in Fig. 4, showed the endo peaks at 108.5 and 152.5 °C. The peak at 152.5 °C corresponds to the melting point. The peak at 108.5 °C shows the thermochromic point and the phase transition energy is estimated to be 6.2 kJ mol^{-1}. The cooling curve shows no endopeak. The X-ray powder diffraction of the red form gives the same diffraction pattern as the powder obtained by heating the violet form. This confirms that the violet form changes to the red form by heating. It should be noted that the behavior of the DSC curve of BPNQ crystal is different from that of the

Table 5. Selected Torsion Angles (τ/°)

Violet form			
C(1)–C(2)–S(1)–C(11)	49.3(5)	C(4)–C(3)–S(2)–C(21)	50.7(5)
C(3)–C(2)–S(1)–C(11)	−141.3(5)	C(2)–C(3)–S(2)–C(21)	−142.5(5)
C(2)–S(1)–C(11)–C(12)	36.9(6)	C(3)–S(2)–C(21)–C(22)	41.0(6)
C(2)–S(1)–C(11)–C(16)	−149.6(5)	C(3)–S(2)–C(21)–C(26)	−148.0(5)
Red form			
C(1)–C(2)–S(1)–C(11)	−49.5(8)		
C(2′)–C(2)–S(1)–C(11)[a)]	−141.0(4)		
C(2)–S(1)–C(11)–C(12)	−60.2(8)		
C(2)–S(1)–C(11)–C(16)	125.6(8)		

a) C(2′) is related by a mirror plane to C(2).

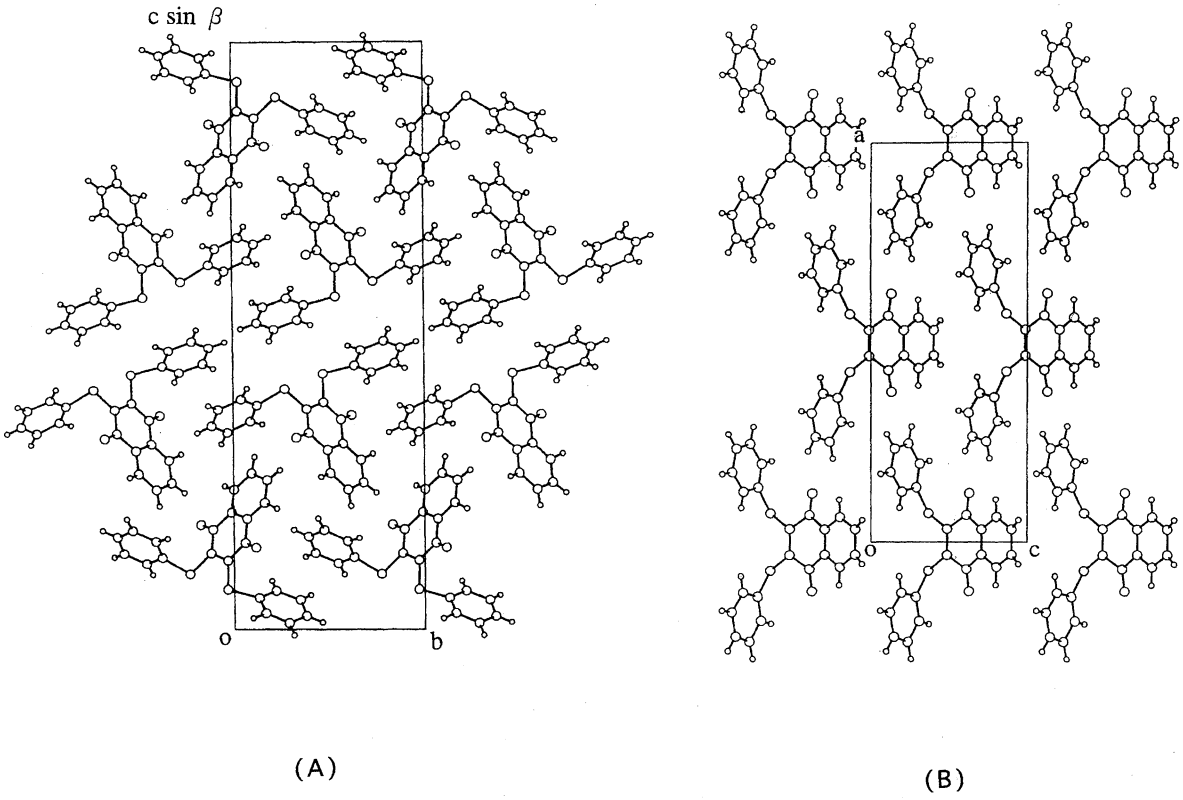

Fig. 3. Molecular arrangement in the crystals: (A) violet form viewed down the *a* axis, (B) red form viewed down the *b* axis.

DSC curve of Cl-BPNQ crystal.[2)] That is, the violet form of BPNQ crystal was found to transform to the red form with an endothermic reaction abruptly at 108.5 °C, although the red crystal of Cl-BPNQ changes slowly to the dark red crystal with an exothermic reaction over the wide temperature range of 145 to 170 °C.[2)]

NMR Studies. Figure 5 shows the Carbon-13 MAS NMR spectra of the red solution of BPNQ in $CDCl_3$. The solution spectrum has a carbonyl carbon C peak at 178.7 ppm and a C(2) carbon peak at 148.3 ppm, and the multi peaks due to the carbon atoms in benzene rings at about 130 ppm. That is, BPNQ molecules in the solution have the C_s symmetry. Figure 6 shows the solid state CP/MAS NMR spectra of the violet and red forms. The spectrum of the red form has a carbonyl carbon C peak at 177.9 ppm and a C(2) carbon peak at 148.1 ppm and the broad peak at 133.2 ppm.

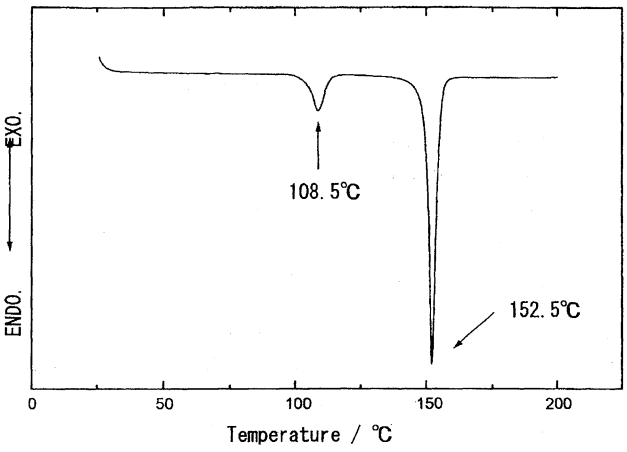

Fig. 4. DSC curve of BPNQ crystals of the violet form.

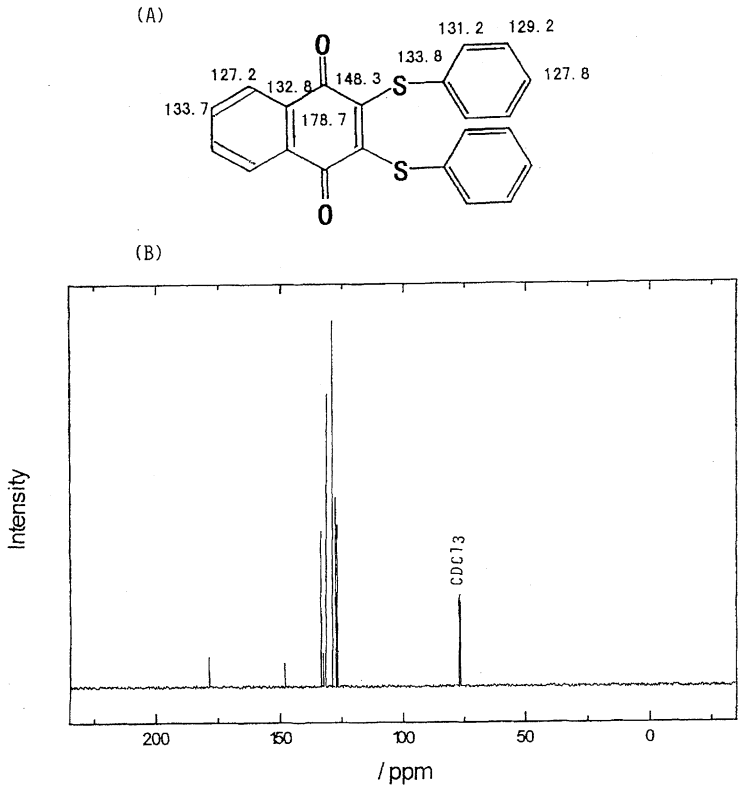

Fig. 5. Carbon-13 MAS NMR spectra of the red solution of BPNQ in $CDCl_3$.

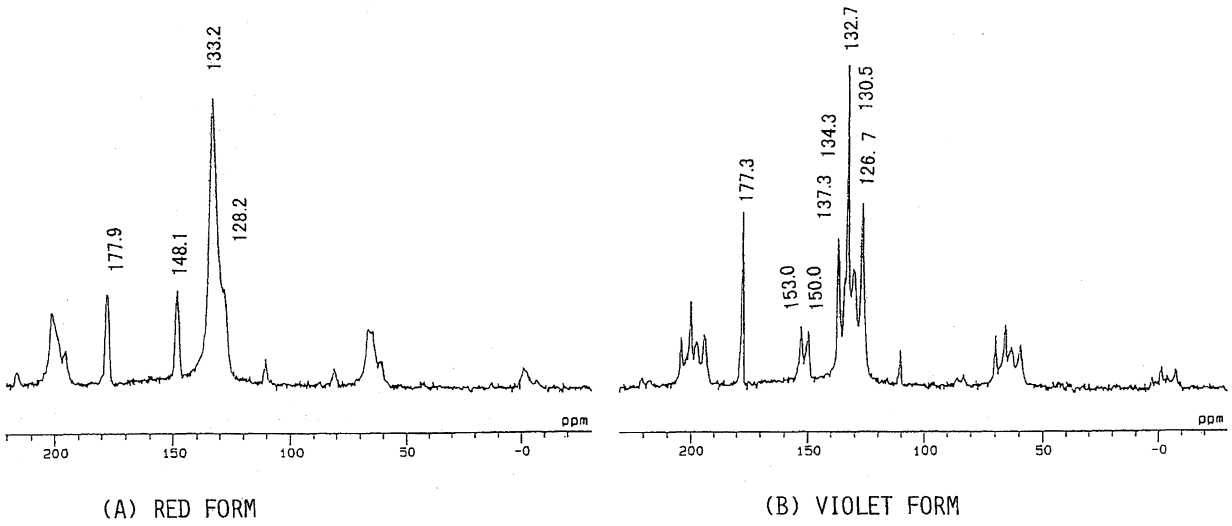

Fig. 6. Solid state CP/MAS NMR spectra of the (A) red and (B) violet forms.

That is, the red solid spectrum shows the same behavior as that of the red solution spectrum except for a few spinning side bands at 200, 70, and 60 ppm. Accordingly, BPNQ molecules in the solution have the same molecular structure as BPNQ molecule in the crystals of red form. On the other hand, the solid state ^{13}C NMR spectrum of the violet form has the single peak at 177.3 ppm of the carbonyl carbon and the doublet at 153.0 and 150.0 ppm due to the carbons at 2 and 3 positions of NQ and the broad peaks at about 130 ppm, except for a few spinning side bands. These results are consistent with the results of the X-ray analysis. The solid state IR and ^{13}C NMR spectra of the red form obtained by the recrystallization has the same pattern as those of the red form transformed by heating. These results are consistent with the results of the X-ray analysis.

Visible Absorption and Theoretical Studies. The solution spectra of NQ and BPNQ are shown in Fig. 7. The spectrum of NQ has two bands at 330 and 250 nm, while the spectrum of BPNQ has two extra bands at 450 and 280 nm in addition to the LE bands of NQ at 330 and 250 nm. Figure 8 shows the visible absorption spectra of the BPNQ crystals. The absorption intensity was estimated from the K-K analysis of the reflection spectra of the crystals.[6] The visible absorption spectrum of the red form has the band at

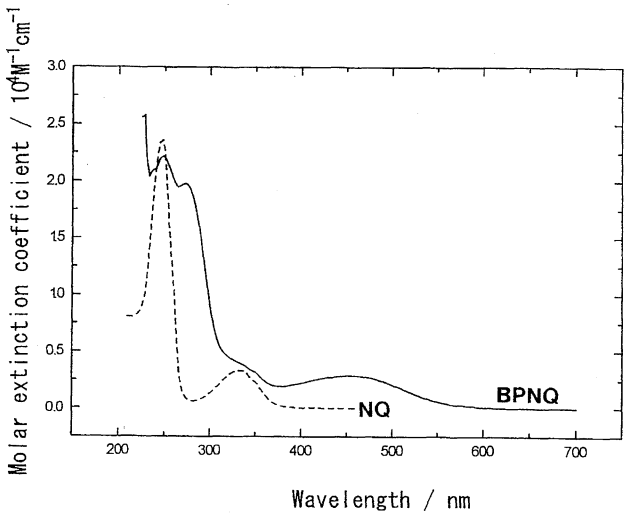

Fig. 7. Solution spectra of NQ and BPNQ.

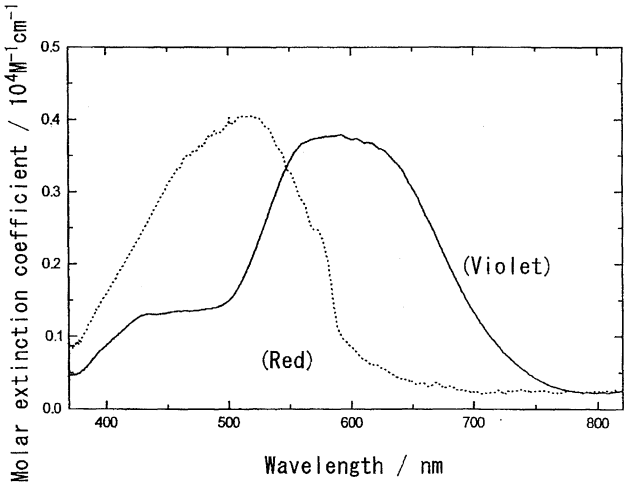

Fig. 8. Visible absorption spectra of the BPNQ crystals.

about 500 nm in addition to the LE band of NQ observed as the shoulder at about 450 nm. That of the violet form has the broad band at 600 nm in addition to the LE band at 450 nm. The comparison of these absorption spectra indicates that the band observed in the crystal spectrum shifts to a longer wavelength region than in the solution spectra. That is, the LE band at 330 nm in the solution appears at 450 nm for both forms, and the 450 nm band in the solution is observed at 500 nm for the red form and at 600 nm for the violet form.

The geometry optimizations with RHF/3-21G* were performed with C_2 symmetry for the violet form and with C_s symmetry for the red form. The total energies of two isomers were calculated by the method of MP2/3-21G*//RHF/3-21G*. The violet form was more stable than the red form in which the energy difference was $\Delta E = 0.4$ kcal mol^{-1}.

Such small energy difference seems to make it possible for the isomerization of BPNQ to occur. Figure 9 shows the orbital energy level diagram with each next-HOMO, HOMO and LUMO of BPNQ molecules for the red and violet forms, and Table 6 shows the lowest allowed excitation energies and its wave functions with the oscillator strengths. The LUMO

Table 6. Lowest Allowed Excitation Energies, Oscillator Strengths, and Wave Functions of BPNQ Molecules in the Violet and Red Forms

	Violet form		Red form	
Excitation energy	4.647 eV		4.967 eV	
Oscillator strength	0.04		0.18	
Wave function				
	88 → 98	−0.1251	87 → 98	0.1049
	94 → 98	0.1718	90 → 98	−0.1752
	97 → 98	0.6030	93 → 98	0.3017
	97 → 100	0.1706	94 → 98	0.1101
	97 → 101	−0.1315	96 → 98	0.5256
			96 → 100	0.1018

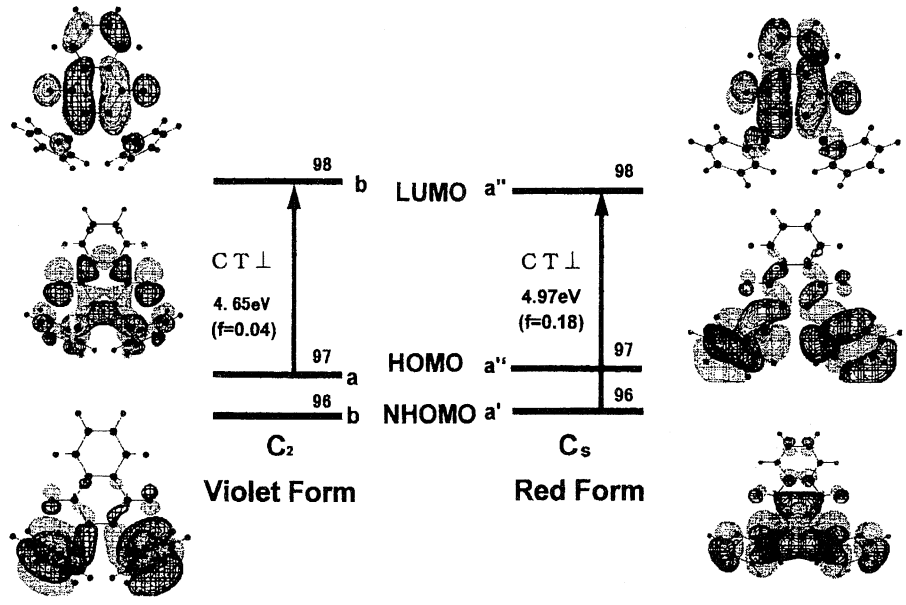

Fig. 9. HOMO, next HOMO, and LUMO orbitals diagrams of BPNQ of the violet and red forms.

is located at NQ, but the HOMO and next HOMO are located at two phenylthio rings. The theoretical analysis shows that the 500 nm band of the red form is assigned to the charge transfer (CT) transition (A″) between the next HOMO (a″) of the phenylthio groups and the LUMO (a′) of the NQ group, and that the 600 nm band of the violet form is assigned to the CT transition (B) between the HOMO (a) of the phenylthio groups and the LUMO (b) of the NQ group.

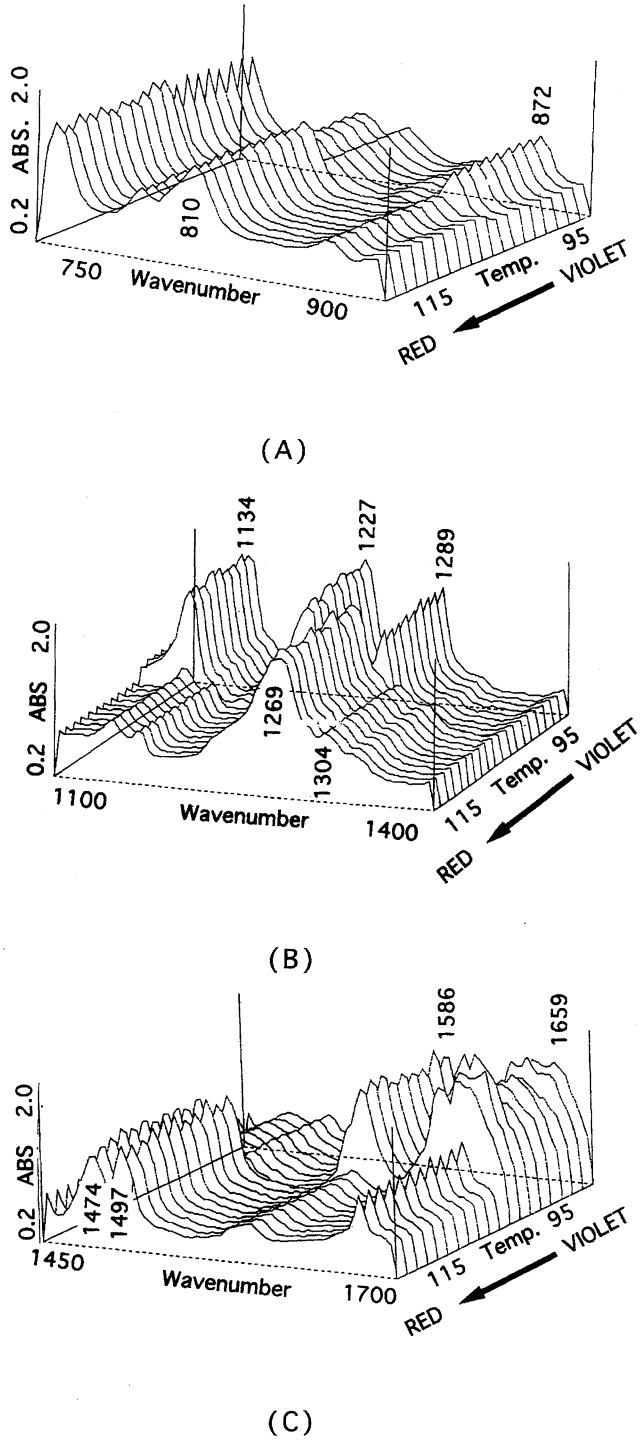

Fig. 10. The Temperature variable IR spectra of the BPNQ crystal.

IR Absorption and Theoretical Studies. Figure 10 shows the temperature variable IR spectra of the red and violet forms of BPNQ crystal. Each peak of the violet form corresponds to each peak of the red form, while some peaks make the red or blue shift and change the absorption intensities suddenly at the phase transition temperature. Such spectral change was observed within 1 degree although the endo peak in the DSC curve has the width of 2 or 3 degrees. This means that the phase transition includes the thermal relaxation process in addition to the variation of the molecular structure. It should be noted that this spectral change is different from those of the phase transition of Cl-BPNQ crystal,[2] while the spectral behaviors of BPNQ and Cl-BPNQ crystals can explain their DSC curves.

Fifteen peaks are observed in the region from 750 to 1700 cm^{-1}, although the BPNQ molecule has 114 vibrational modes on these conformations. The IR vibronic frequencies was calculated with RHF/3-21G* method. These calculated values are comparable with the experimental ones by multiplying 0.89 to the computed frequencies and the difference between the calculated frequencies for the red and violet forms is small. The calculated vibrational frequencies show that IR active CO stretching mode at 1900 cm^{-1} appears as the antisymmetric type in the violet form, and symmetric type in the red form. The broad band observed at 1659 cm^{-1} for the violet form and the sharp peak at 1667 cm^{-1} for the red form can be assigned to the CO stretching mode.

Conclusion. The BPNQ crystal has the sharp transition temperature and shows the chromic phenomenon from the violet form to the red form. That is, the BPNQ material has the posibility to be used for the on-off devices like the CD-WORM (Write Once Read Memory) or the temperature indicator.

References

1) G. R. Desiraju, I. C. Paul, and D. Y. Curtin, *J. Am. Chem. Soc.*, **99**, 1594 (1977).

2) H. Hayashi, M. Tanaka, S. Matsumoto, S. Kashino, and K. Mogi, *Mol. Cryst. Liq. Cryst.*, **286**, 305 (1996).

3) M. Tanaka, H. Matsui, J. Mizoguchi, and S. Kashino, *Bull. Chem. Soc. Jpn.*, **67**, 1572 (1994).

4) K. Miyaki and N. Ikeda, *Yakugaku Zasshi*, **73**, 964 (1953).

5) L. H. Fieser and R. H. Brown, *J. Am. Chem. Soc.*, **71**, 3609 (1949).

6) M. Tanaka, "The 4-th Jikken Kagakukouza," ed by K. Yoshihara, Maruzen, Tokyo (1992), Vol. IV, p. 2298.

7) The complete $F_o - F_c$ data are deposited as Document No. 70005 at the Office of the Editor of Bull. Chem. Soc. Jpn.

8) G. J. Gilmore, *J. Appl. Crystallogr.*, **17**, 42 (1984).

9) "International Tables for X-Ray Crystallography," Kynoch Press, Birmingham (Present distributor Kluwer Academic Publisher, Dordrecht) (1974), Vol. IV, pp. 22—98.

10) "TEXAN. Single Crystal Structure Analysis Software, Version 5.0," Molecular Corporation, The Woodlands, Texas (1989).

11) M. J. Frisch, G. W. Trucks, H. B. Schlegel, P. M. W. Gill, B. G. Johnson, M. A. Robb, J. R. Cheeseman, T. Keith, G. A. Petersson, J. A. Montgomery, M. A. Al-Laham, V. G. Zakrzewski, J. V. Ortiz, J. B. Foresman, J. Cioslowski, B. B. Stefanov, K. Raghavachari,

A. Nanayakkara, M. Challacombe, C. Y. Peng, P. Y. Ayala, W. Chen, M. W. Wong, J. L. Andres, E. S. Replogle, R. Gomperts, R. L. Martin, D. J. Fox, J. S. Binkely, D. J. Defrees, J. Baker, J. P. Stewart, M. Head-Gordon, C. Gonzalez, and J. A. Pople, "Gaussian 94, Revision C," Gaussian, Inc., Pittsburgh, PA, USA (1995).

12) C. K. Johnson, "ORTEP II, Report ORNL-5138," Oak Ridge National Laboratory, Tennessee (1976).

13) P. J. Gaultier and C. Hauw, *Acta Crystallogr.*, **23**, 1016 (1967).

14) P. M. Breton-Lacombe, *Acta Crystallogr.*, **23**, 1024 (1967).